Electronic Supplementary Material (ESI) for Dalton Transactions.

Supplementary Information for

Tailoring the local environment around metal ions: solution chemical and structural study of some multidentate tripodal ligands†

Ferenc Matyuska[a], Attila Szorcsik[b], Nóra V. May[c], Ágnes Dancs[a], Éva Kováts[d], Attila Bényei[e] and Tamás Gajda[a,b,*]

[a] *Department of Inorganic and Analytical Chemistry, University of Szeged, Dóm tér 7, H-6720 Szeged, Hungary. E-mail: gajda@chem.u-szeged.hu*
[b] *MTA-SZTE Bioinorganic Chemistry Research Group, Dóm tér 7, H-6720 Szeged, Hungary*
[c] *Research Centre for Natural Sciences HAS, Magyar tudósok körútja 2, H-1117 Budapest, Hungary*
[d] *Institute for Solid State Physics and Optics, Wigner Research Centre for Physics HAS, Konkoly Thege Miklós u. 29-33, H-1121 Budapest, Hungary*
[e] *Department of Pharmaceutical Chemistry, University of Debrecen, Egyetem tér 1, Debrecen H-4032, Hungary*

Contents:

Table S1. Selected hydrogen bond distances and angles in the crystal structure **1**,**2**,**3** and DOSVAI [18] and CAFXEN [19]

D*—H···*A	***D*—H (Å)**	**H···*A* (Å)**	***D*···*A* (Å)**	***D*—H···*A* (°)**
[Zn(tachpyr)] × $(ClO_4)_2$ × O (1)				
N1—H1···O6^{i}	0.98	2.08	2.988(8)	154
N1A—H1A···O3^{ii}	0.98	2.10	3.031(7)	159
N1B—H1B···O1	0.98	2.54	3.509(8)	172
C3—H3B···O4^{ii}	0.97	2.57	3.426(7)	147
C5B—H5B···O5^{iii}	0.93	2.54	3.435(8)	162
C6—H6···O6^{iv}	0.93	2.48	3.348(11)	156
C7—H7···O8^{iv}	0.93	2.45	3.20(2)	138
C3B—H3B2···O7^{iii}	0.97	2.41	3.333(19)	159
[Zn(tachpyr)] × (ClO_4) × Cl (2)				
N1—H1N···Cl2	0.98	2.16	3.105(3)	161
C2—H2B···Cl2	0.97	2.77	3.563(4)	140
C8—H8···O2	0.93	2.51	3.18(2)	129
[Zn(tachpyr)] × $(ClO_4)_2$ × (CH_3OH) [18]				
N1—H1···O1^{v}	0.808(6)	2.343(6)	3.096(6)	155.4(4)
C5—H7···O3^{vi}	0.951(8)	2.484(6)	3.352(4)	151.8(6)
C7—H9···O3^{vi}	0.950(8)	2.552(7)	3.421(7)	152.3(6)
[Cu(tachpyr)] × $(ClO_4)_2$ × H_2O (3)				
N1—H1···O6	0.89 (2)	2.11 (4)	2.956 (9)	158 (5)
N1A—H1A···O3	0.90 (6)	2.30 (6)	3.041 (12)	140 (5)
N1B—H1B···O1^{vii}	0.91 (3)	2.56 (3)	3.454 (13)	170 (6)
C3—H3B···O4	0.97	2.50	3.353(12)	147
C5B—H5BO···O5^{viii}	0.93	2.54	3.454(11)	168
C6—H6···O6^{ix}	0.93	2.53	3.411(12)	159
C7—H7···O8^{ix}	0.93	2.53	3.260(19)	136
C3B—H3B2···O7^{viii}	0.97	2.41	3.357(17)	167
[Cu(tachpyr)] × $(ClO_4)_2$ × 0.5(C_2H_3N) [19]				
N1—H1···O6^{x}	1.06	2.31	3.352	169
N1A—H1A···O3^{xi}	0.96	2.21	3.039	143
N1B—H1B···O1^{xii}	0.99	2.09	3.053	165
C7—H14···O8^{x}	0.99	2.52	3.420	150
C9—H15···O2^{xiii}	0.95	2.49	3.427	171
C16—H22···O1^{xii}	0.85	2.52	3.461	171
C13—H20···O7^{xiii}	0.99	2.40	3.295	151

Symmetry codes : ^{i}1/2+x,1/2-y,-1/2+z , ^{ii} 3/2-x,1/2+y,1/2-z, ^{iii} 1/2-x,-1/2+y,1/2-z, ^{iv} 1/2-x,1/2+y,1/2-z, ^{v}-3/2-y,-1-z,1/2+x, ^{vi} -1-y,-3/2+z,-1/2-x, ^{vii} 3/2-x,-1/2+y,3/2-z, ^{viii} 2-x,1-y,2-z, ^{ix} 3/2-x,-1/2+y,3/2-z, ^{x}1/2-x,-1/2+y,1/2-z, ^{xi}1-x,1-y,-z, ^{xii}1+x,y,z, ^{xiii}x,-1+y,z,

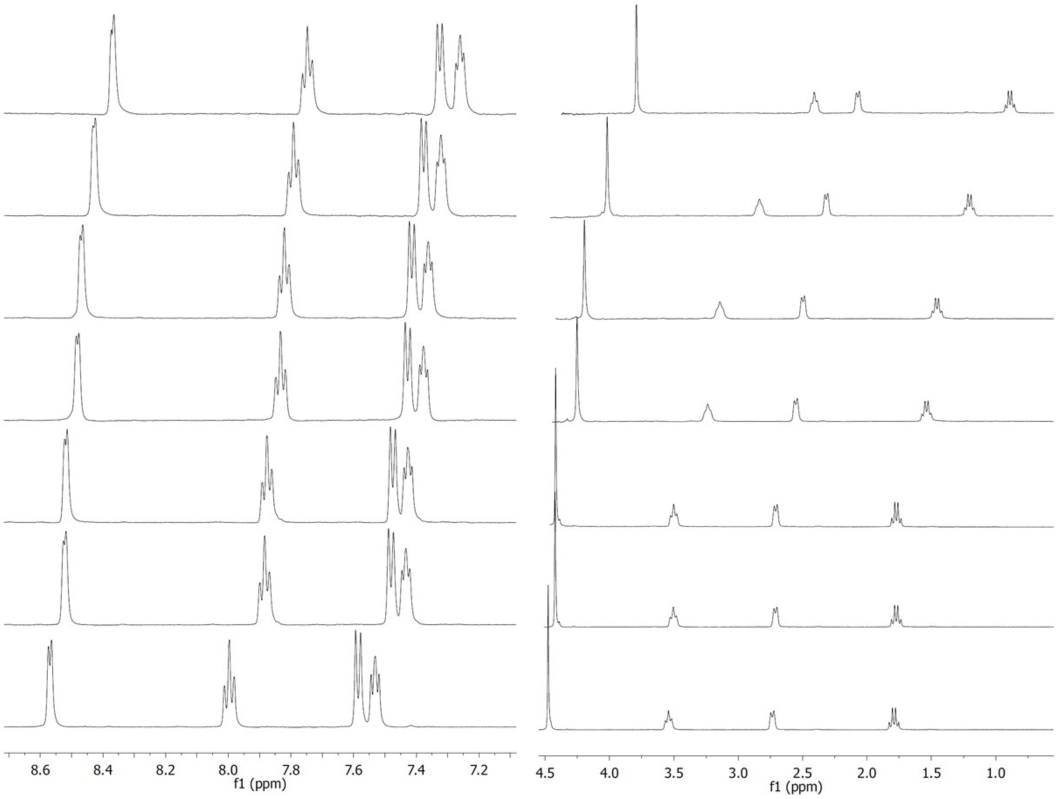

Figure S1. The pH-dependent ^{1}H-NMR spectra of tachpyr (0.003 M, 298 K, in 10% D_2O-H_2O, pH (bottom up) = 1.59, 2.78, 3.25, 5.67, 6.17, 7.54)

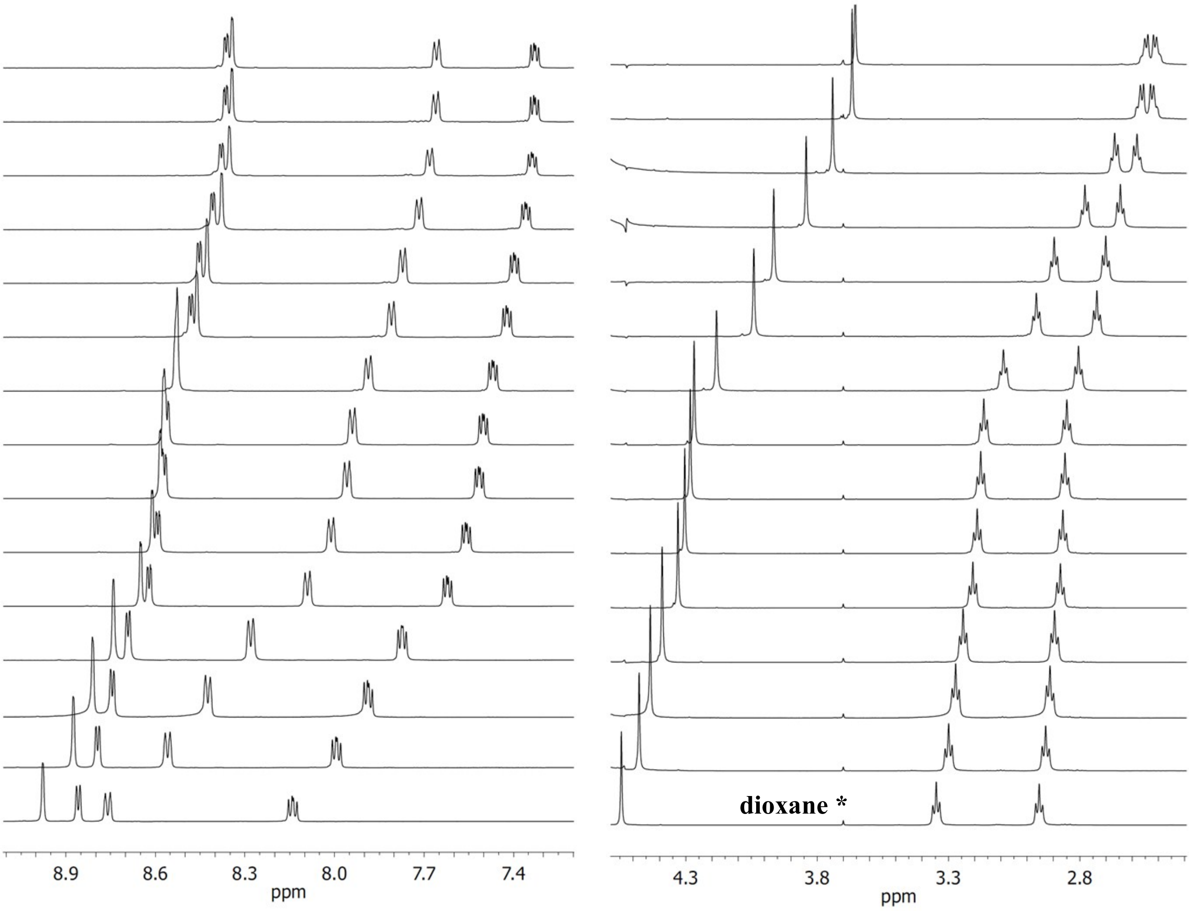

Figure S2. The pH-dependent ^{1}H-NMR spectra of tren3pyr (0.003 M, 298 K, in 10% D_2O-H_2O, pH (bottom up) = 1.27, 2.26, 2.55, 2.98, 3.70, 4.12, 4.72, 5.41, 6.21, 7.01, 7.46, 8.09, 8.74, 10.79)

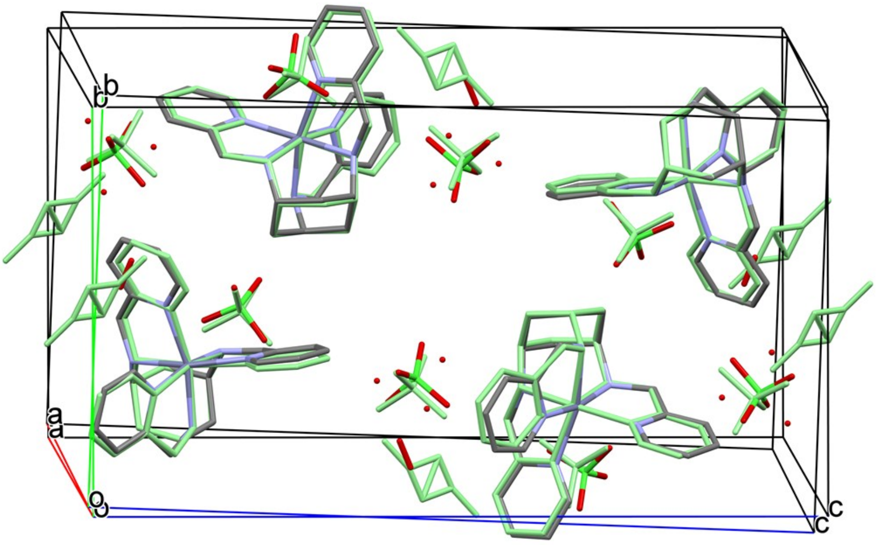

Cell Similarity Index (π):

$$\pi = |(a+b+c)/(a'+b'+c')-1| \tag{1}$$

where *a, b, c,* and *a', b', c'* are the orthogonalized lattice parameters of the related crystals. In the event of great similarity of the two unit cells, π is close to zero.

Isostructurality Index (*I(s)*):

$$I_i(n) = \left| \left[\frac{\Sigma(\Delta R_i)^2}{n} \right]^{1/2} - 1 \right| * 100 \tag{2}$$

where *n* is the number of distance differences between the crystal coordinates (ΔR_i) of identical non-H atoms within the same section of the related structures. *I(s)* takes into account both the differences in the geometry of the molecules and the positional differences caused by rotation and translation.

Figure S3. Comparison of the unit cells of [Zn(tachpyr)] × $(ClO_4)_2$ × O (**1**) colored (by element) and [Cu(tachpyr)] × $(ClO_4)_2$ × 0.5(C_2H_3N) CAFXEN [19] (green). The cyclohexane rings of the four cations in the unit cell are superimposed. Equations (1) and (2) shows the calculation of cell similarity and isostructurality indices ((A. Kálmán, L.Párkányi and Gy. Argay, *Acta Crystallogr. Sect. B*, 1993, **49**, 1039-1049; A. Kálmán and L. Párkányi: Isostructurality of Organic Crystals in *Advances in Molecular Structure Research*, Vol.3, M. Hargittai & I. Hargittai (editors), pp. 189-226 (1997). JAI Press Inc.).

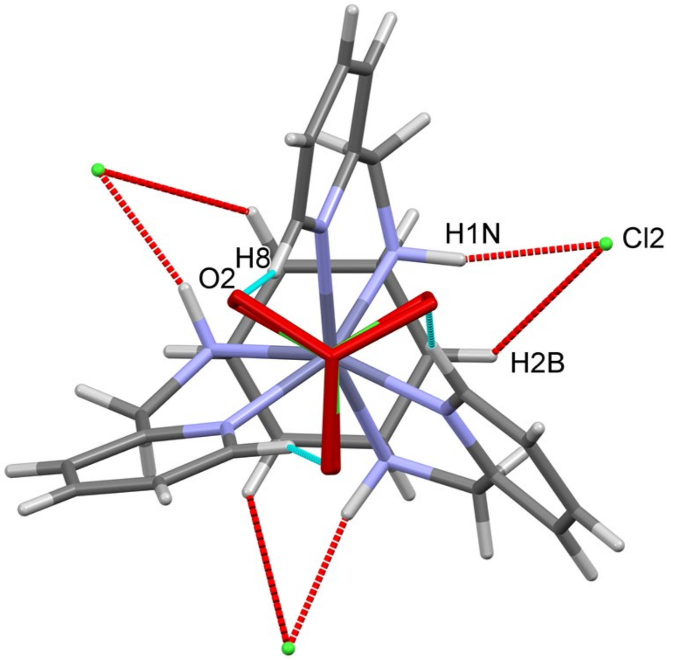

Figure S4. Symmetrical (C_3) molecular and hydrogen bond arrangement of [Zn(tachpyr)] in crystal **2** (*R*-3*c*).

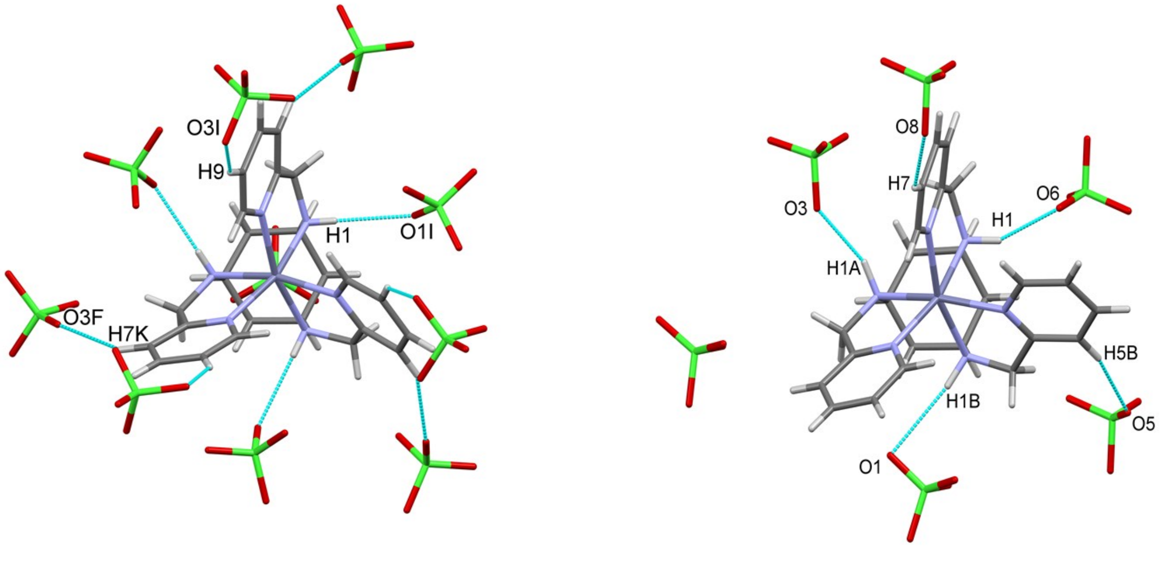

Figure S5. Left: symmetrical (C_3) hydrogen bond arrangement of the [Zn(tachpyr)] in the crystal DOSVAI [18] ($P2_13$); Right: The asymmetric hydrogen bond arrangement of the [Zn(tachpyr)] in the crystal **1** ($P2_1/n$)

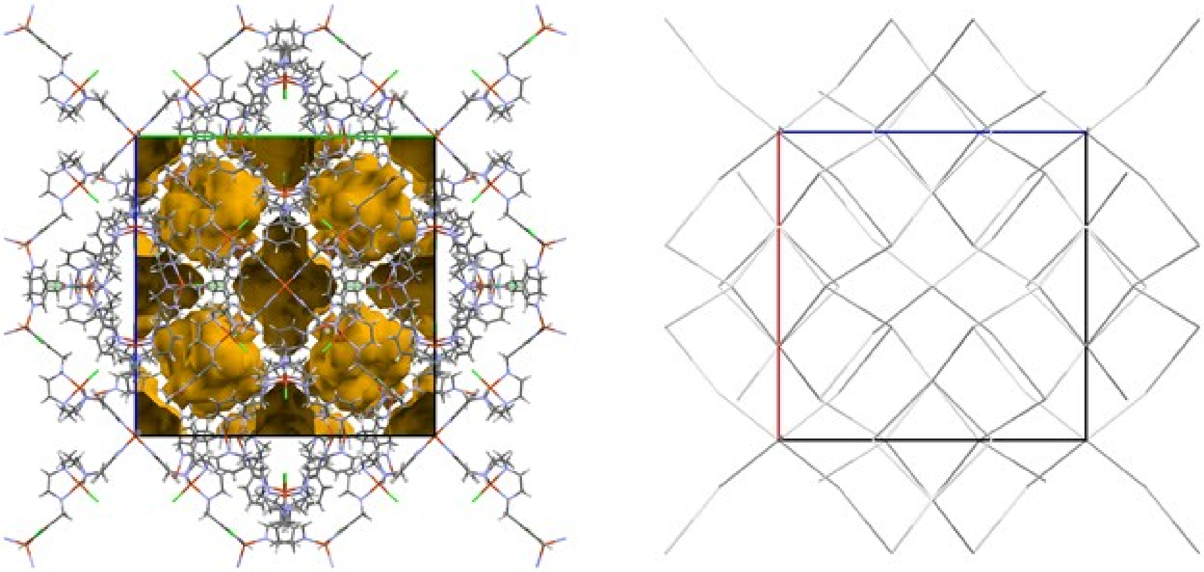

Figure S6. Left: Crystal structure and voids of Cu-ten3pyr polymer. Solvent molecules and counter ions are omitted for clarity. Yellow shapes represent the voids between the two interpenetrated polymer networks; their total volume is 20.8% of the unit cell volume. Right: Simplified topology of the crystal structure. The topology classification is 3,3,4-c net based on calculation with ToposPRO 5.1.0.7 (V.A. Blatov, A.P. Shevchenko, D.M. Proserpio *Cryst. Growth Des*. (2014), 14, 3576-3586.)

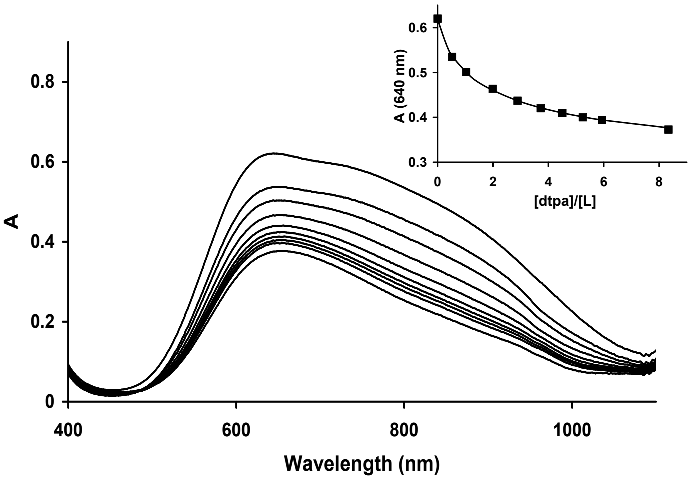

Figure S7. Displacement of of the ligand from Cu(trenpyr) by diethylenetriamine pentaacetic acid (dpta) (pH = 10.0, $[Cu^{2+}]$ = [trenpyr] = 1.74 mM). Insert shows the changes of absorbance at 640 nm. The protonation and complex formation constants of dtpa are log β_{011} = 10.54, log β_{011} = 19.1, log β_{011} = 23.4, log β_{011} = 26.17, log β_{011} = 28.17, log β_{011} = 21.5, G (Anderegg, F. Arnad-Neu, R. Delgado, J. Feldman, K. Popov, Pure Appl. Chem., 77 (2005) 1445-1495.)

.

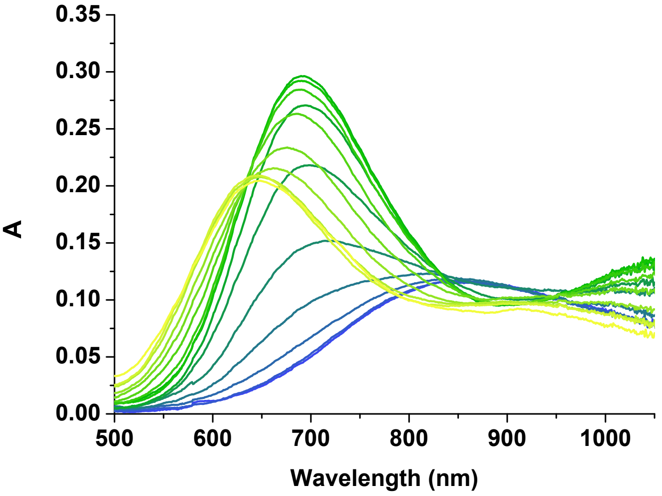

Figure S8. Effect of pH on the Vis/NIR spectra of the copper(II)-tach3pyr systems (T = 298 K, I = 0.1 M NaCl, $[Cu^{2+}]$ = [tach3pyr] = 0.00226 M, pH = 3.5 – 9.8 from blue to yellow).

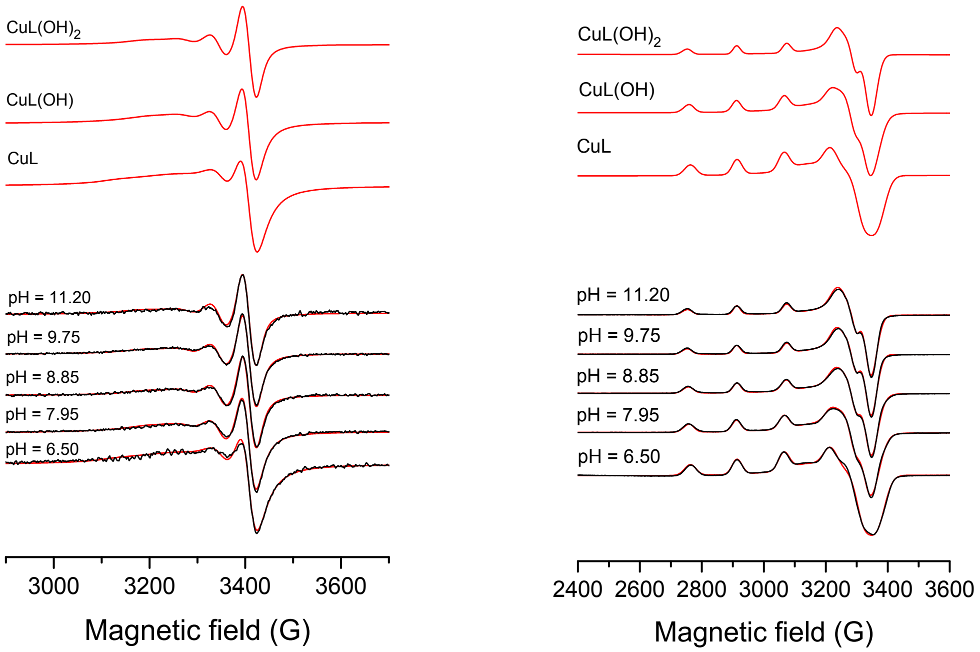

Figure S9. Experimental (black) and simulated (red) EPR spectra of the copper(II)-tach3pyr system at room temperature (left) and at 77 K (right) in 60% (w/w) dmso-water ($[Cu^{2+}]$ = [tach3pyr] = 2.6 mM). The calculated component spectra of the main species are also shown on the top.

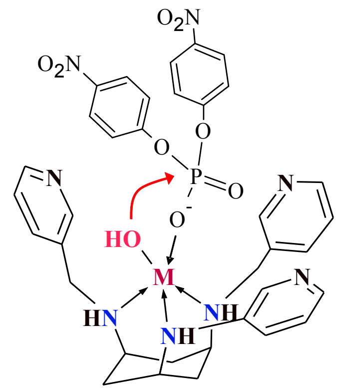

Figure S10. Schematic mechanism of Cu(tach3pyr)(OH) promoted hydrolysis of bnpp

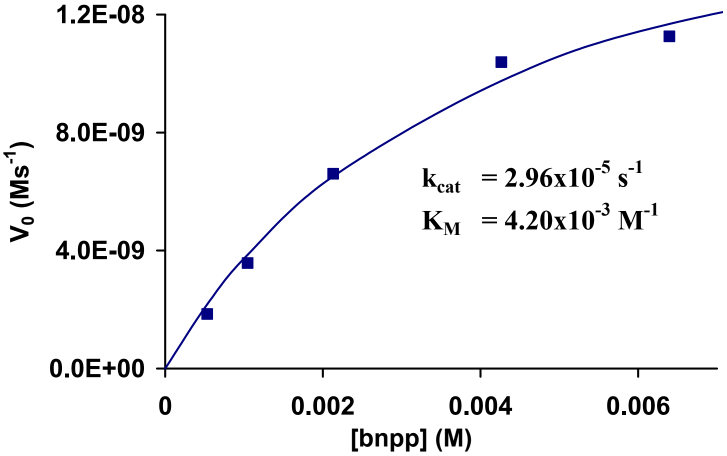

Figure S11. Saturation kinetic experiments for the hydrolysis of bnpp promoted by Cu(tach3pyr)(OH) ([Cu^{2+}] = [tach3pyr] = 0.6 mM, pH = 8.7 in 60% (w/w) dmso-water)).

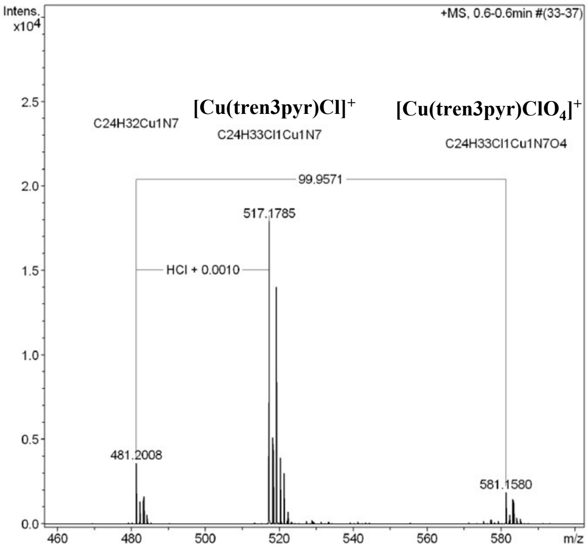

Figure S12. MS spectrum of the Cu(II)-tren3pyr 1/1 system at pH 7 indicating the presence of mononuclear complexes

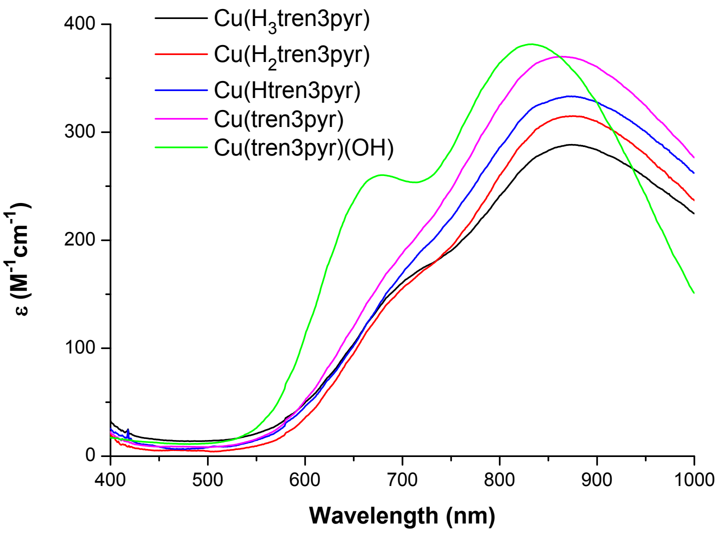

Figure S13. Individual molar Vis/NIR spectra of copper(II)-tren3pyr complexes

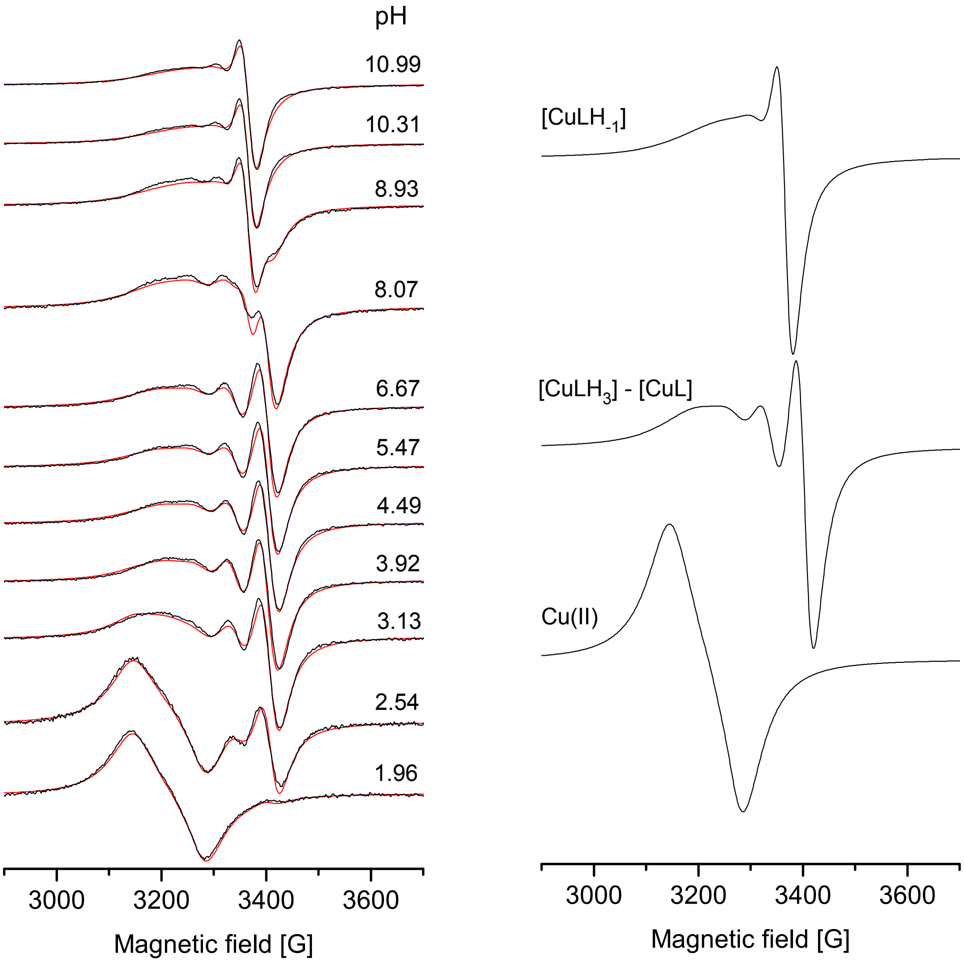

Figure S14. Experimental (black) and simulated (red) EPR spectra of the copper(II)-tren3pyr system at room temperature ($[Cu^{2+}]$ = [tren3pyr] = 2 mM). The calculated component spectra of the main species are also shown in the right.

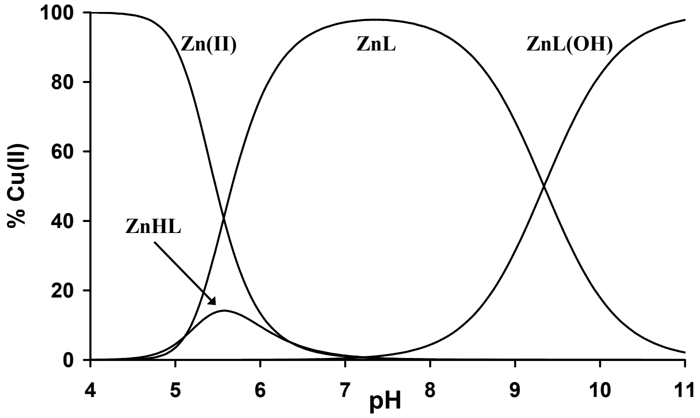

Figure S15. Speciation diagram of the zinc(II)-tren3pyr complexes ($[Zn^{2+}]$ = [tren3pyr] = 0.002 M, T = 298 K, I = 0.1 M NaCl).